ACS Catalysis

Research Article

pubs.acs.org/acscatalysis

Operando Studies of the Catalytic Hydrogenation of Ethylene on Pt(111) Single Crystal Surfaces

Aashani Tilekaratne, Juan Pablo Simonovis, Maria Francisca López Fagúndez,† Maryam Ebrahimi, and Francisco Zaera*

Department of Chemistry, University of California, Riverside, Riverside, California 92521, United States

ABSTRACT: The hydrogenation of ethylene on Pt(111) single-crystal surfaces was studied by combining measurements of the kinetics of reaction using mass spectrometry detection with the simultaneous characterization of the species present on the surface using reflection–absorption infrared spectroscopy. The kinetics measured by us matches past reports on the same system, with zero- and first-order dependence on the partial pressures of ethylene and hydrogen, respectively, and extensive H–D exchange if D_2 is used instead of H_2. The reaction takes place in the presence of an alkylidyne surface layer, which forms immediately upon exposure of the clean surface to the reaction mixture and can be removed by hydrogen or another olefin but at rates 1–2 orders of magnitude slower than the ethylene-to-ethane conversion. The nature of the alkylidyne surface species changes slightly upon being exposed to high pressures of hydrogen, with the carbon in the terminal methyl moiety acquiring some sp^2 character. Moreover, the alkylidyne hydrogenation rate shows an inverse relationship with H_2 pressure and is reduced by the presence of olefins in the gas phase. Turnover frequencies for the olefin hydrogenation reaction under pressures in the Torr range are high, as reported repeatedly in the past, but the corresponding reaction probabilities are quite low, below the 10^{-4} range. In contrast, almost unit reaction probability was observed here in effusive collimated molecular beam experiments emulating intermediate pressure conditions.

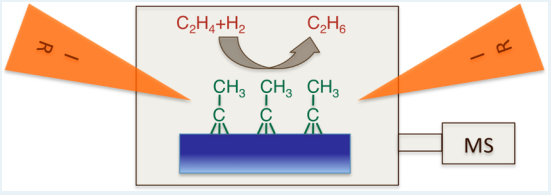

KEYWORDS: *olefin hydrogenation, infrared absorption spectroscopy, mass spectrometry, kinetics, platinum, high-pressure cell, kinetics, alkylidynes*

1. INTRODUCTION

The in situ characterization of the solid surfaces of the catalysts during heterogeneous catalysis is central to the understanding of the mechanism of the catalyzed reactions. This is certainly the case with hydrocarbon conversion reactions catalyzed by transition metals, for which it is known that the active surface is covered with strongly bonded hydrocarbon fragments.[1] The understanding of the mechanism of olefin hydrogenation reactions promoted by late transition metals such as platinum has already benefitted considerably from such an approach.[2,3] The first mechanistic insights on these systems were derived from traditional kinetic experiments using supported catalysts and typical heterogeneous catalytic reactors.[4] On the basis of the kinetic parameters measured this way[5,6] and isotopic labeling and isotopic analysis of the products,[7−9] a basic mechanism was proposed in which hydrogenation takes place on the surface of the metal in a stepwise manner, and the formation of an adsorbed alkyl intermediate is followed by two competing pathways, the reverse β-hydride elimination back to the olefin and the incorporation of the second hydrogen atom to produce the alkane.

This so-called Horiuti–Polanyi mechanism[10] is, in fact, still used to this day to describe the basic features of these reactions.[11,12] However, data from ^{14}C radiolabeling,[13] infrared absorption spectroscopy,[14] and NMR[15] experiments, among others, soon provided evidence to suggest that these hydrogenation reactions are not as simple as first thought, and that they take place on surfaces covered by strongly bonded hydrocarbon fragments. It was even suggested that hydrogenation on metals may occur not by direct hydrogen addition from the surface to the olefin but, rather, via an intermediate hydrogen transferring step involving the adsorbed hydrocarbons.[16] Although this view is no longer favored, the role of the hydrocarbon fragments is still in dispute. What has become clear is that the mechanism of catalytic olefin hydrogenation reactions is complex and needs to incorporate side decomposition steps and the participation of coadsorbed hydrocarbon species.[17]

In parallel, a better molecular-level understanding of the thermal chemistry of olefins on transition metal surfaces, on platinum in particular, has been advanced by the use of modern surface-sensitive techniques in studies under controlled ultrahigh vacuum (UHV) environments and with well-defined single-crystal surfaces.[18−20] A complex series of reactions was established this way for olefins adsorbed on many single-crystal surfaces, on Pt(111) in particular.[3,21,22] Not only was it proven that it is possible to promote a small production of alkanes from alkenes even under vacuum either with or without

Special Issue: Operando and In Situ Studies of Catalysis

Received: June 25, 2012
Revised: July 23, 2012
Published: September 27, 2012

   dx.doi.org/10.1021/cs300411p | *ACS Catal.* 2012, 2, 2259–2268

coadsorbed hydrogen, but it was also shown that the main reaction pathway for the adsorbed olefin around room temperature is the formation of an alkylidyne surface species in which one of the terminal carbon atoms sits on a 3-fold hollow site, triply bonded to the metal, and an alkyl moiety is bonded to that carbon.[23−25] In the case of ethylene, for instance, adsorption at about room temperature results in the saturation of the surface with a quarter of a monolayer of ethylidyne ($Pt_3{\equiv}CCH_3$, the coverage defined relative to the number of surface Pt atoms). The mechanism of formation of these alkylidyne surface species has been (and still is) hotly debated,[26−37] but most research groups believe it involves an ethylidene ($Pt_2{=}CHCH_3$) intermediate.[30,38−42] Such alkylidene species may contribute to the olefin hydrogenation mechanism either by participating in the hydrogen transfer steps mentioned above or, more likely, by removing or temporarily displacing the alkylidyne from the metal sites required for olefin hydrogenation.

As this molecular-level picture of the chemistry of olefins on clean metal surfaces developed, though, it also became clear that such chemistry, which is seen under vacuum, does not necessarily reflect what takes place during catalytic reactions. First, it was found that there are, in fact, two forms by which olefins bind to metal surfaces: one involving the rehybridization of the carbon−carbon double bond and the formation of two Pt−C sigma bonds and the other via an interaction between the π electrons of the olefin and the d orbitals of the metal.[43−46] Although di-σ bonding is stronger and occurs first on clean surfaces (except at very low temperatures), it leads to the formation of alkylidynes, and it is likely not directly involved in the catalytic hydrogenation of the olefins. Instead, it is the π-bonded species that is believed to be the intermediate for those reactions.[47−50] It should be noted that there are, in fact, two types of π-bonded olefins, an intrinsic precursor to the formation of the di-σ species on clean metals,[51,52] and an extrinsic precursor that forms on hydrogen- or hydrocarbon-precovered surfaces;[47,49,53,54] it is the latter that is the one relevant for catalysis. How the π-bonded olefin undergoes the hydrogen incorporation steps that lead to the production of the alkane is still not fully understood.[55]

More recently, thanks to the development of the so-called high-pressure cell by which the samples may be transferred between a UHV chamber and a small catalytic reactor without exposing them to the outside atmosphere,[56−58] it has been possible to carry out reactivity studies on single-crystal surfaces under realistic catalytic conditions. Using this approach, the solid sample can be cleaned and thoroughly characterized before reaction and also analyzed immediately after their catalytic performance.[59,60] In the case of ethylene hydrogenation on Pt(111) (and Rh(111) surfaces), a series of post-mortem characterization experiments were used to establish that, indeed, the species present on the surface during catalysis are ethylidyne moieties.[61−64] Later studies involving in situ spectroscopic characterization of the surface while in the catalytic environment have corroborated the validity of this conclusion, both on single-crystal surfaces[49,65] and with supported catalysts[66,67]

Our present understanding of olefin hydrogenation processes catalyzed by transition metals retains the basic features of the Horiuti−Polanyi mechanism, but adds the fact that the reactions take place on a surface almost fully covered with hydrocarbon fragments, specifically alkylidyne moieties, and that they start with a weakly bonded π-bonded species. However, many questions remain unanswered still.[68] First, it is not clear how those π-bonded olefin molecules, presumably adsorbed on a second layer on top of the alkylidyne fragments, react with the hydrogen atoms, which are adsorbed directly on the metal. As mentioned above, it has been suggested that the carbonaceous layer may shuttle the H atoms from the metal to the olefins on the second layer,[16,69] but evidence for this is not available, and such process seems highly unlikely.[20,46] Alternatively, the alkylidyne species could be in dynamic equilibrium with the coadsorbed hydrogen, possibly transitorily forming alkylidene moieties or other intermediates and diffusing to adjacent sites (such as bridged 2-fold ensembles) and opening space for the incoming π-bonded olefins so that they can pick up surface hydrogen.[46,70] It is also not clear how the transition takes place in terms of reaction kinetics between the surface chemistry seen under vacuum, where strong olefin adsorption and decomposition on the clean metal surface is followed by its passivation and where no steady-state olefin-to-alkane conversion is ever achieved, and the catalytic regime observed under atmospheric pressures, where the reaction occurs under mild conditions and with high turnover frequencies (but not necessarily high reaction probabilities). Here we describe our initial experiments using a newly developed operando setup to try to address these issues.

2. EXPERIMENTAL DETAILS

The core ultrahigh vacuum (UHV) apparatus used in these studies has been described in previous publications.[71,72] This two-tier stainless-steel chamber is pumped to a base pressure of approximately 1×10^{-10} Torr by using a cryopump. The main level is used for sample cleaning, which is performed by a combination of argon ion bombardment, annealing, and thermal treatments with O_2 to burn any remaining surface carbon contaminants. A UTI 100C quadrupole mass spectrometer (MS) retrofitted with a retractable nose cone terminated in a 5-mm-diameter aperture is available for temperature-programmed desorption (TPD) experiments, but was used here mainly to analyze the gas mixtures during the course of the catalytic reactions performed in the high-pressure cell (see below). This mass spectrometer is interfaced to a personal computer capable of recording full mass spectra of the gases in the UHV chamber in the 1−300 amu range or, alternatively, monitoring the time evolution of up to 15 chosen masses as a function of time.

The second level of this chamber, accessible by using a horizontal long-travel manipulator, is set up to perform reflection−absorption infrared spectroscopy (RAIRS) experiments. The IR beam from a Bruker Equinox 55 Fourier-transform infrared (FT-IR) spectrometer is directed through a polarizer, made to travel inside the UHV chamber through a NaCl window, and focused at grazing incidence (~85°) onto the sample by using a long focal length (12 in.) parabolic mirror. The reflected beam is then collected, after going through a second NaCl window, by a similar second parabolic mirror and focused onto a narrow-band mercury−cadmium−telluride (MCT) detector. The entire beam path is enclosed in a sealed box purged with dry air and purified by using a scrubber (Balston 75-60) for CO_2 and water removal. All spectra were acquired by averaging the data from 2000 scans taken at a resolution of 4 cm^{-1}, a process that takes about 4 min per experiment, and ratioed against spectra from the clean sample obtained in the same way but before gas dosing. Spectra

dx.doi.org/10.1021/cs300411p | ACS Catal. 2012, 2, 2259−2268

were taken with both s- and p-polarized light to discriminate between gas-phase and adsorbed species.[73,74]

A retractable small high-pressure cell was added to this second tier of the UHV chamber to carry out the catalytic experiments. The general design of our cell is similar to that reported in the past,[56−58] but new features were added to allow for the characterization of the surface by RAIRS simultaneously during catalytic reactions under atmospheric pressures, in operando mode. A cylindrical cup, approximately 2 in. in diameter and 2 in. in depth (∼42 mL total inside volume), was mounted on a separate linear translation stage designed to bring the cell in and out of the position used for the RAIRS data acquisition. The end of this cup was retrofitted with a Viton O-ring, which can be pressed against the flat surface of a second cylinder mounted on the sample manipulator, behind the platinum sample, to enclose the crystal in the small cell volume and isolate it from the vacuum environment. A 1/2-in.-diameter tube was attached to the other end of the cell for gas feeding and gas pumping, which was done by using a manifold equipped with a pressure gauge and a small (∼50 L/s) turbopump. Two small NaCl windows were added at opposite sides of the lateral walls of the main body of the cell to allow for the IR beam to travel in and out of the reactor volume to acquire RAIRS data in situ while exposing the platinum crystal to atmospheric pressures. Images of this high-pressure cell (dismounted) and of the end of the manipulator used to hold and translate the sample between the two tiers of the UHV chamber and to seal the high-pressure cell are provided in Figure 1. A small leak persists between the high-pressure cell and the UHV chamber when in the closed (high-pressure reaction) position because of incomplete sealing by the O-ring. That leak, which causes the pressure in the UHV chamber to rise to approximately 3.5×10^{-7} Torr upon filling the high-pressure cell with 100 Torr of H_2, was used to analyze the composition of the gas mixture in the cell continuously versus reaction time by using the mass spectrometer.

The effusive molecular beam experiment reported in Figure 9 was carried out in a second UHV chamber turbopumped to a base pressure of about 1×10^{-9} Torr and equipped with an ion gun for sample cleaning and another UTI 100C quadrupole mass spectrometer interfaced to a personal computer, as in the first chamber, for data collection.[58] The effusive molecular beams were generated by pressurizing the back of a capillary tube, 150 μm in diameter and 1.2 cm in length, with atmospheric pressures of the reaction mixture (made out of prefixed partial pressures of C_2H_4 and H_2). The beam flux was controlled by using a leak valve placed between the gas supply and the capillary, and followed by recording the pressure drop in the gas reservoir (a 0.5 L glass bulb filled to ∼200 Torr of the reaction mixture) versus time using a capacitance manometer. A polycrystalline polished Pt disk was mounted on an on-axis vertical manipulator capable of $X−Y−Z−\theta$ motion, and the sample was positioned within a few micrometers of the outlet of the capillary doser during the hydrogenation experiments. The beam was deemed to be fairly collimated by experiments in which the spots produced by condensation of thick layers of heavy hydrocarbons on the Pt surface at low temperatures were inspected visually as a function of distance; similar-sized spots were observed even after retracting the sample several centimeters away from the doser. Further experiments are underway to better characterize the flux and angular distribution of our beam.

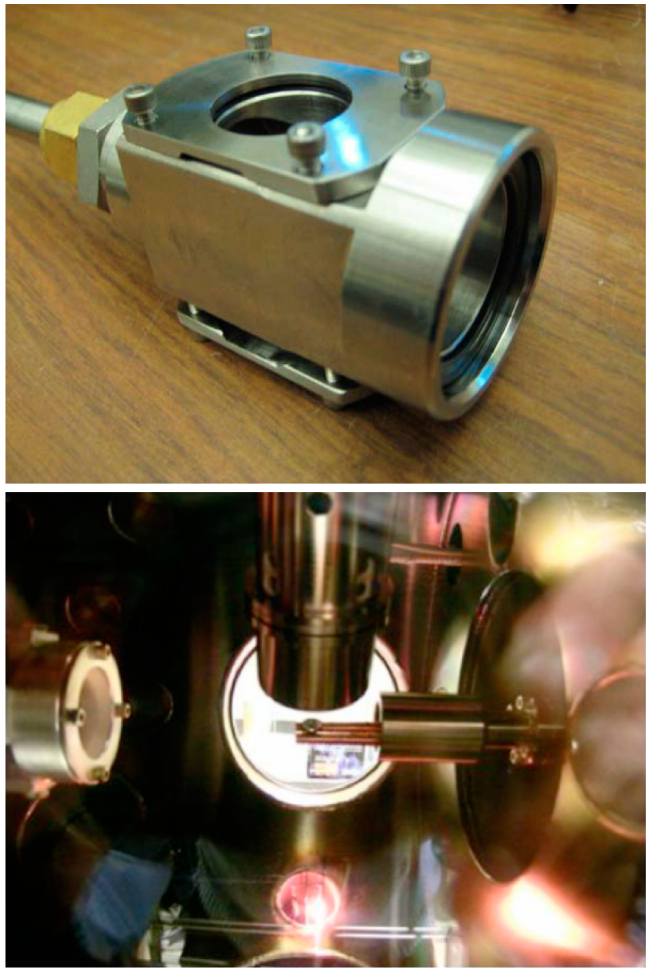

Figure 1. Pictures of the high-pressure cell (top) and overall arrangement (bottom) used in the operando studies. Top: high pressure cell, which consists of a small cylindrical cup fitted with an O-ring (right) to make a seal when pressed against the cylindrical piece of the manipulator and has two NaCl windows retrofitted to the side walls to let the infrared beam in and out of the cell during reaction (the holder for one of those windows is shown here on top). Also shown is the gas feeding and pumping tube placed at the back of the cell. Bottom: holding arrangement for the Pt crystal inside the UHV chamber, showing the stainless steel cylinder used to seal the high-pressure cell (right) and the two copper rods used to hold the sample. The cylindrical piece seen on the right of the bottom picture is used to guide the manipulator to the RAIRS position in the UHV chamber.

In both systems, the platinum samples, a Pt(111) single crystal in the MS-RAIRS chamber and a Pt polycrystalline piece in the molecular beam apparatus (both in the shape of disks ∼9 mm in diameter and 1.5 mm in thickness) were spotwelded to a pair of tantalum wires attached to the copper electrical feedthroughs of the sample manipulators (Figure 1). This arrangement allows for the crystals to be cooled to ∼100 K by using liquid nitrogen (by continuously flowing the liquid nitrogen through the air side of the feedthroughs in the first chamber, where the manipulator is in a horizontal position, and simply by filling the liquid reservoir in the second, vertical, arrangement) and to be heated resistively to up to 1100 K. The temperature of the samples is measured by using a chromel−alumel thermocouple spotwelded to their side and controlled by using homemade feedback electronics. The gases were purchased from commercial sources (H_2 from Liquid Carbonic

dx.doi.org/10.1021/cs300411p | ACS Catal. 2012, 2, 2259−2268

(>99.995% purity); D_2 (>99.5% atom purity), C_2H_4 (99.5%), and C_3H_6 (>99% purity) from Matheson; and C_2D_4 and C_3D_6 from Cambridge Isotope Laboratories (both 99% D purity)) and were used as supplied.

3. RESULTS

The kinetics of the catalytic hydrogenation of ethylene on Pt(111) surfaces was followed by mass spectrometry by analyzing the small amount of gas that leaks from the high-pressure cell into the UHV chamber. Examples of the sequence of mass spectra recorded as a function of reaction time are provided in Figure 2 for the reaction of normal ethylene, C_2H_4,

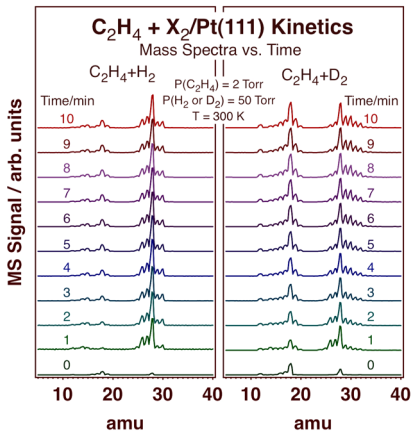

Figure 2. Mass spectra of the reaction mixture as a function of reaction time recorded during two catalytic hydrogenation experiments using a Pt(111) single-crystal surface as the catalyst, starting with 2 Torr of normal ethylene and 50 Torr of either H_2 (left) or D_2 (right). All reactions were carried out at 300 K. Hydrogenation is indicated by the appearance of peaks at 29 and 30 amu in the left panel, and extensive H−D exchange by the signals seen at higher mases in the right panel.

with either H_2 (left panel) or D_2 (right panel). Mixtures of 2 Torr of ethylene and 50 Torr of hydrogen (or deuterium) were used, and the reactions were carried out at room temperature (300 K). To follow the progress of these reactions, particular focus was placed on the evolution of the signals in the 25−36 amu range. In the case of hydrogenation with regular hydrogen gas (left panel), ethane formation is indicated mainly by the growth of the peaks at 29 and 30 amu; the signals for 26, 27, and 28 amu contain contributions from both ethylene and ethane and need to be deconvoluted to extract information about the partial pressures of each compound.[58,75] If D_2 is used instead of H_2 (right panel), the evolution of $C_2H_4D_2$, the main expected product, can be followed by measuring the signal intensity for 32 amu, its molecular weight; however, the mass spectra in this case are more complex, also showing peaks at higher masses.

In general, it can be seen from these raw data that complete hydrogenation occurs within only a few minutes of reaction and that some H−D exchange also takes place if isotopic labeling is used. The identity of the ethylene and ethane in the gas phase were also corroborated in situ by taking infrared absorption spectra of the gas-phase mixture inside the high-pressure cell during reaction (data not shown). The spectra from the adsorbed versus gas-phase species could be separated by using a well-known surface selection rule that applies to RAIRS on metal surfaces, by taking data using both s- and p-polarized light.[73,74] The time resolution of the kinetic data obtained this way was not as good as that from mass spectrometry detection because each pair of IR spectra (with s- and p-polarized light) requires approximately 10 min of acquisition time, but the results obtained were fully consistent with those reported in Figure 2. Blank experiments were also carried out with a dirty crystal to make sure that no catalytic activity was promoted by any other surface in the reactor; no significant conversion was detected in the time frame of our experiments.

Data such as those in Figure 2 can be analyzed quantitatively by deconvoluting the raw signals using known mass spectrometry cracking patterns for all the reactants and products, in this case for all the possible isotopomers of ethane (eleven) and ethylene (six).[76,77] However, because there are not enough peaks in the mass spectra to cover all possible products and because the cracking patterns of some of these molecules are quite similar, some approximations need to be made in the analysis. In our study, two main approximations were made: (1) all stereoisomers of a given isotopomer (i.e., CHD=CHD and CD_2=CH_2, etc.) were treated as one single species, and (2) some of the ethylene isotopomers that require extensive isotopic scrambling prior to hydrogenation (or deuteration) were neglected (i.e., C_2D_4, C_2D_3H, and $C_2D_2H_2$ in the case of C_2H_4 + D_2). With those approximations and following a deconvolution procedure described elsewhere,[58,75] the data in the right panel of Figure 2 were converted into a plot of conversion versus time for all the products; the results are shown in Figure 3.

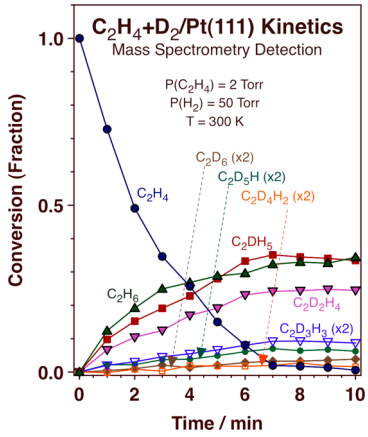

Figure 3. Kinetics of reaction for the case of the C_2H_4 + D_2 mixture shown in the right panel of Figure 1. The raw data was deconvoluted by using a reported procedure to identify the different isotopomers of ethylene and ethane.[58] Extensive H−D exchange is manifested by the large production of C_2DH_5 and C_2H_6, and as many as four H−D substitutions in the original ethylene (the maximum possible) is indicated by the detection of all ethane isotopomers, all the way to C_2D_6.

It can be seen that, in this example, hydrogenation (deuteration) is complete after less than <7 min and that extensive and multiple H−D exchange takes place. It is known that the isotopic scrambling occurs within the initial ethylene molecules because, once formed, ethane cannot be activated and readsorbed on the surface under the conditions of these experiments.[4,5,78] That prior reaction is sufficiently extensive here, to the extent that the expected product from straight deuteration of C_2H_4, $C_2D_2H_4$, is not even the main product from the deuteration steps. Indeed, the yield for the dideutero isotopomer amounts to only ∼25% of the total ethane

dx.doi.org/10.1021/cs300411p | ACS Catal. 2012, 2, 2259−2268

produced, and C_2DH_5 and C_2H_6 dominate the product mixture, instead. All other possible ethane isotopomers were detected as well, all the way to C_2D_6, indicating (again) the extensive nature of the isotopic scrambling in the original ethylene. However, no C_2H_3D could be identified within the detection limits of these experiments, a result that supports our approximation of neglecting the other ethylene isotopomers in the analysis, and that suggests that hydrogenation (deuteration) is fast and may directly involve the surface intermediates also responsible for the isotopic exchange. All these observations are consistent with additional data obtained using $C_2D_4 + H_2$ and $C_2D_4 + D_2$ mixtures (not shown) and also with previous reports on this system.[61]

Making use of our operando setup, the nature of the surface species adsorbed on the surface of the Pt(111) crystal was characterized by RAIRS simultaneously during the course of the ethylene hydrogenation catalytic reaction. The left panel of Figure 4 shows an example of the data obtained, in this case a

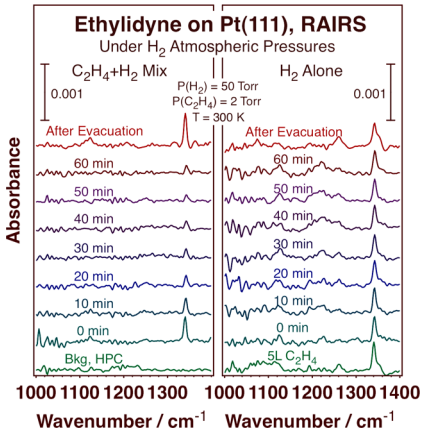

Figure 4. Reflection–absorption infrared spectroscopy data as a function of time for the species formed on the Pt(111) surface upon immersion into atmospheric pressure environments. Two examples are reported here for exposure of a clean Pt(111) surface to a mixture of ethylene and hydrogen (left) and for the treatment of a saturated ethylidyne layer, preprepared by saturation with ethylene at room temperature under UHV, with an atmosphere of pure hydrogen (right). In both cases, the signature peak for ethylidyne at ~1340 cm^{-1} is seen, and small changes in frequency and intensity because of the gas-phase treatments are also observed.

set of RAIRS traces in the 1000–1400 cm^{-1} range recorded as a function of reaction time during the hydrogenation of 2 Torr of C_2H_4 with 50 Torr of H_2 at room temperature. These spectra are dominated by a peak at about 1340 cm^{-1} and a smaller feature sometimes identifiable at 1120 cm^{-1}. Together with a third feature at 2885 cm^{-1}, these vibrational frequencies are easily assigned to the methyl symmetric deformation (umbrella, $\delta_s(CH_3)$), C–C stretching (ν(C–C)), and methyl C–H stretching ($\nu_s(CH_3)$) modes of ethylidyne, a species well-known to form upon adsorption of ethylene on clean Pt(111) and other surfaces.[24,71,79,80] It is also well-known that such alkylidyne species form on the Pt(111) surface under olefin catalytic hydrogenation conditions; their presence has already been detected in situ by both infrared absorption spectroscopy[49,58,81] and sum frequency generation.[47] Our data are consistent with those previous reports.

One interesting observation deriving from the data in Figure 4 is that the frequencies of the main peaks identified with the alkylidyne surface species shift to higher values, by a few wavenumbers, upon exposure to atmospheric pressures of the reactants. In fact, this is the case even in pure hydrogen atmospheres, in the absence of any gas-phase olefin in the mixture (Figure 4, right panel). This observation turned out to be quite general: blue shifts were seen for the methyl symmetric stretching ($\delta_s(CH_3)$) and C–C stretching (ν(C–C)) modes of normal and perdeutero ethylidyne, respectively, and also for the methyl asymmetric stretching ($\nu_{as}(CH_3)$ and $\nu_{as}(CD_3)$) of normal and perdeutero propylidyne (made via room-temperature adsorption of propylene under UHV).[53] The frequency-shift data are summarized in Table 1. These shifts are consistent

Table 1. Frequency (ω) Shifts in Vibrational Modes Associated with Alkylidyne Species Adsorbed on Pt(111) Single-Crystal Surfaces upon Exposure to Atmospheric Pressures of Hydrogen

system	vibrational mode	ω/cm^{-1} (UHV)	$\Delta\omega$/cm^{-1}
C_2H_3/Pt(111) + H_2[a]	$\delta_s(CH_3)$	1339.6 ± 0.5	2.7 ± 0.7
C_2H_3/Pt(111) + D_2[a]	$\delta_s(CH_3)$	1339.6 ± 0.5	2.9 ± 0.7
C_2H_4+H_2/Pt(111)[b]	$\delta_s(CH_3)$	1339.6 ± 0.5	2.7 ± 0.7
C_2D_3/Pt(111) + H_2[a]	ν(CC)	1145.1 ± 0.5	6.4 ± 0.7
C_2D_4+H_2/Pt(111)[b]	ν(CC)	1145.1 ± 0.5	5.4 ± 0.7
C_3H_5/Pt(111) + H_2[a]	$\nu_{as}(CH_3)$	2960.6 ± 0.5	6.2 ± 0.5
C_3D_5/Pt(111) + H_2[a]	$\nu_{as}(CD_3)$	2223.3 ± 0.5	3.1 ± 0.5

[a]A saturated alkylidyne layer was first prepared by exposure of the clean Pt(111) surface to 40 L of the olefin at 300 K under UHV conditions, then the surface was inserted into the high-pressure cell and exposed to 100 Torr of hydrogen. [b]A clean Pt(111) surface was inserted into the high-pressure cell and exposed to a mixture of 2 Torr of the olefin and 100 Torr of hydrogen.

with binding either to a more electronegative surface (because of the effect of adsorbed hydrogen) or with terminal methyl moieties with more sp^2 character. Regarding the latter explanation, the vibrational frequency values seen for the alkylidynes under hydrogen atmospheres are between numbers from the same alkylidynes under vacuum and frequencies reported for analogous iodoalkanes.[71,82] It can be argued that coadsorption of hydrogen atoms on the surface modifies the electronic properties of the platinum and, with that, the nature of the bonding to the alkylidyne surface species.

Another piece of information worth extracting from the data in Figure 4 is the kinetics of removal of the alkylidyne surface species upon exposure to atmospheric pressures of the reactants. In general terms, the IR signals from those species decrease with time, albeit at a relatively slow rate, much slower than that for the hydrogenation of the olefin.[46,64] Note, for instance, that whereas full conversion of 2 Torr of ethylene with hydrogen or deuterium occurs within a few minutes (<7 min) of reaction in the experiments reported in Figures 2 and 3, significant ethylidyne coverages are detected by RAIRS in Figure 4 even after 1 h of exposure to the gases. It should be pointed out that in these experiments the conversion of the olefin was often faster than the time resolution we could achieve in the RAIRS experiments: each set of RAIRS traces required ~10 min for the data acquisition. Nevertheless, important differences could still be detected between experiments with the reaction mixture versus with hydrogen alone (see below).

The kinetics of the alkylidyne removal is summarized in Figure 5 for three cases: for ethylidyne in the presence of either

dx.doi.org/10.1021/cs300411p | ACS Catal. 2012, 2, 2259–2268

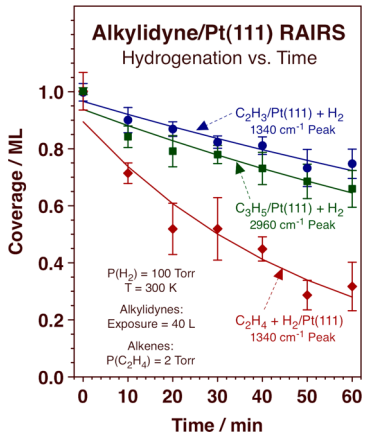

Figure 5. Time evolution of the coverage of alkylidyne species adsorbed on the Pt(111) surface in high-pressure environments, as measured by the time dependence of the intensity of the appropriate peaks in the RAIRS spectra, for three different cases, namely, (a) for a predosed ethylidyne layer exposed to pure hydrogen (blue circles), (b) for the ethylidyne layer that forms upon exposing the clean surface to a mixture of ethylene and hydrogen (red diamonds), and (c) for a predosed layer of propylidyne exposed to pure hydrogen (green triangles). Slow ethylidyne removal is seen in both cases, at rates much slower than those for olefin hydrogenation, and faster removal rates are measured if the gas contains an olefin.

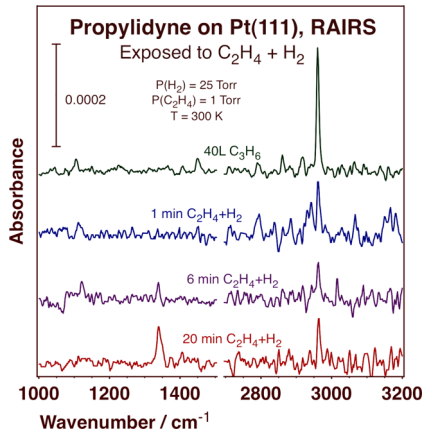

Figure 6. RAIRS from a saturated propylidyne layer, prepared by propylene adsorption under UHV, during exposure to a mixture of 1 Torr of ethylene and 25 Torr of hydrogen. Spectra are shown for three different exposure times. The coverage of propylidyne, identified by the feature at 2960 cm^{-1}, decreases slowly with time as it becomes replaced, at last in part, by a new layer of ethylidyne (the peak at 1340 cm^{-1}).

pure hydrogen (100 Torr) or C_2H_4 + H_2 mixtures (2 + 100 Torr), and for propylidyne in the presence of pure hydrogen (100 Torr). A couple of observations can be extracted from these data: (1) the rates of removal of ethylidyne and propylidyne with pure H_2 are comparable; and (2) the rate of ethylidyne removal is faster with ethylene + hydrogen mixtures relative to those measured with hydrogen alone. This last conclusion seems counterintuitive, because it could be argued that when ethylene is present in the gas phase, it should be possible for the ethylidyne removed from the surface to be replaced with fresh surface species. One possible explanation may be that the observed trend is the result of a physical effect, a decrease in IR signal due to increase disorder on the surface (because of collisions or interactions with gas-phase ethylene); the full ethylidyne IR signal strengths are regained after evacuation (Figure 4, left panel). On the other hand, it is also possible that the hydrogenation of the adsorbed ethylidyne requires a relatively large ensemble of surface atoms and that those may be partially blocked by hydrogen. In this picture, overcrowding of the surface with hydrogen in the presence of high pressures of H_2 may slow down the ethylidyne conversion because of a poisoning effect due to surface site blocking. The presence of the olefin in the gas mixture may partially inhibit the hydrogen surface uptake, leading to less overcrowding of those surface sites and allowing for more room for the ethylidyne to react and ultimately desorb from the surface. The inverse pressure dependence of alkylidyne surface removal with hydrogen pressure reported later in this report is consistent with that interpretation.

An alternative way to follow the kinetics of removal of the surface alkylidyne species during olefin hydrogenation catalysis is to start with a different adsorbed alkylidyne, by predepositing a different olefin under UHV conditions, and then following the rate of its replacement in situ by RAIRS during the catalytic olefin hydrogenation process. An example of the data obtained using this approach is provided in Figure 6, in this case for a Pt(111) surface saturated with propylidyne prior to its exposure to a C_2H_4 + H_2 mixture. Both the disappearance of propylidyne and the formation of ethylidyne (by conversion of ethylene from the gas phase) on the surface could be followed by measuring the intensities of the 2960 ($\nu_{as}(CH_3)$ in propylidyne) and 1340 ($\delta_s(CH_3)$ ethylidyne) cm^{-1} peaks, respectively. It is clear that the exchange of these alkylidynes (propylidyne by ethylidyne) on the surface starts at early reaction times, since a significant decrease in the population of surface propylidyne is seen even after only 1 min of reaction. This initial drop in intensity could perhaps be related to the physical phenomenon mentioned above, but, in any case, there is also a clear increase in ethylidyne coverage with reaction time: after 20 min of reaction, the coverages of ethylidyne and propylidyne on the Pt(111) surface are comparable (the peak intensities of both peaks can be compared directly because their IR cross sections are similar). The extent of propylidyne removal in this case is comparable to that reported for ethylidyne in the presence of C_2H_4 + H_2 mixtures in Figure 5 and, again, faster than what is seen if the surface is immersed in an atmosphere of pure hydrogen.

The rate of ethylene hydrogenation on the propylidyne-precovered Pt(111) surface was followed simultaneously by mass spectrometry during the RAIRS surface characterization experiments for alkylidyne exchange discussed in the previous paragraph. In fact, to obtain better kinetic data, the signals for specific masses versus time rather than complete mass spectra were acquired. In Figure 7, the accumulation of ethane in the reaction cell, measured by following the signal for 30 amu, is shown as a function of reaction time for the case of ethylene hydrogenation with H_2 on propylidyne presaturated Pt(111) single-crystal surfaces. Data are reported for five different initial pressures of hydrogen, ranging from 10 to 50 Torr (the initial pressure of ethylene was kept the same in all cases, at 2 Torr). One thing that becomes evident from these results is that, in the cases where high excesses of hydrogen are used, the rate of ethane formation displays approximately zero-order kinetics (the rate of ethane production, the slopes of the plots in Figure 7, are constant versus time all the way to reaction completion). Only when lower hydrogen pressures are used are deviations

dx.doi.org/10.1021/cs300411p | ACS Catal. 2012, 2, 2259−2268

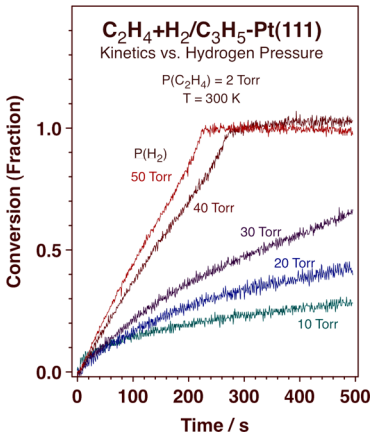

Figure 7. Kinetics of accumulation of ethane in the high-pressure cell, from ethylene hydrogenation, followed by the mass spectrometry signal intensity for 30 amu and reported in terms of conversion fraction versus time, as a function of the partial pressure of hydrogen (the initial partial pressure of ethylene was kept constant at 2 Torr in all cases). These reactions were carried out on propylidyne presaturated Pt(111) surfaces, the same as in Figure 6. Because the cell acts as a batch reactor, the straight lines seen with high hydrogen pressures indicate zero-order kinetics in ethylene. Approximately first-order kinetics in hydrogen was also estimated from the initial rates of reaction, extracted from the slopes of these traces (see Figure 8).

from such behavior seen. Since this pseudo-zero-order kinetics is seen under an excess of hydrogen, it must be ascribed to the ethylene: its pressure in the reaction mixture does not affect the reaction rate, at least under the conditions of these experiments. On the other hand, higher hydrogen initial pressures clearly lead to faster reaction rates. Quantitative analysis of the initial reaction rates, estimated from the slopes of these traces at $t = 0$ s and reported in Figure 8, yielded a kinetic reaction order on

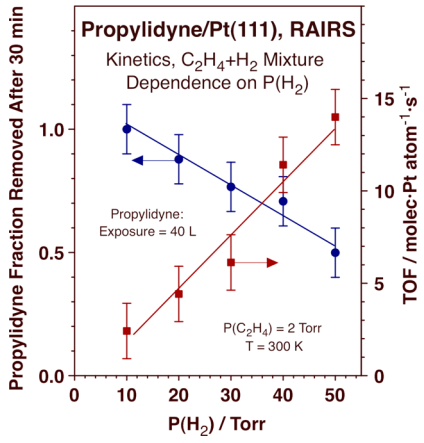

Figure 8. Initial turnover frequencies for ethylene hydrogenation to ethane (red squares) and extent of propylidyne removal from the Pt(111) surface after 30 min of reaction (blue circles) as a function of hydrogen partial pressure. Counterintuitively, the rate of propylidyne removal decreases with increasing hydrogen pressure.

hydrogen partial pressure (the slope of a plot of ln(TOF) versus $\ln(P_{H_2})$) of 1.2 ± 0.1. The kinetic parameters measured in the experiments reported here are consistent with values reported previously for both Pt(111) single crystals[61] and Pt-supported catalysts.[5]

The kinetics of the replacement of the initial propylidyne layer on the Pt(111) single-crystal surface by the new ethylidyne layer formed upon exposure to C_2H_4 + H_2 reaction mixtures was also characterized by RAIRS as a function of H_2 pressure. The extent of the removal of the propylidyne surface species after 30 min of reaction at 300 K, as estimated from the intensity of the 2960 cm^{-1} peak, is reported for several hydrogen pressures in Figure 8. A clear monotonic decrease in the extent of this removal was observed with increasing H_2 pressure. This is perhaps an unexpected trend, but one consistent with that seen in Figure 5. Again, we suggest that an excess of hydrogen gas may result in a high coverage of atomic hydrogen coadsorbed with the alkylidyne on the surface and that such surface crowding may partially inhibit the hydrogenation of the surface carbonaceous species. What is interesting here is that, according to the data in Figure 8, the rate of olefin hydrogenation does increase with hydrogen pressure; it is only the surface species that follow the reverse trend.

Finally, we briefly discuss the kinetics of these catalytic hydrogenation reactions in terms of reaction probabilities. Olefin hydrogenations catalyzed by late transition metals such as platinum are considered facile and, indeed, display relatively high turnover frequencies (TOF), even at low temperatures.[4,83] The initial TOF values reported in Figure 8 range from about 2.4 molecules/(Pt atom·s) for 10 Torr of H_2 to about 14 molecules/(Pt atom·s) for the case of 50 Torr of H_2, close to those reported previously on Pt(111) surfaces.[61] However, in terms of probabilities, these numbers are still relatively low, on the order of 10^{-5} ethylene conversions/collision. Given that the reaction kinetics is zeroth order in ethylene pressure, though, the expectation is that such probability should increase in an inversely proportional way with decreasing olefin pressure. This means that reaction probabilities may reach reasonably high values for ethylene pressures on the order of submilli-Torr. Of course, this inverse proportionality cannot hold in the low-pressure extreme, since below ~10^{-5} Torr, it would imply that the reaction probabilities can reach values above unity. Not only would that be physically unreasonable, but it is known that catalytic reactions cannot be sustained under ultrahigh vacuum at all,[48] except perhaps in the case of palladium nanoparticles.[84,85] Nevertheless, there should be an intermediate pressure regime in which these catalyzed olefin hydrogenation reactions are quite efficient.[58] Unfortunately, it is experimentally difficult to explore such a pressure regime with the existing high-pressure cell setups. Instead, in Figure 9, we show preliminary results from an alternative molecular beam experiment, using a capillary arrangement, designed to obtain high local fluxes of the reactants on the platinum surface under UHV conditions.[74,86] As predicted, reaction probabilities close to unity were observed. We are presently calibrating our system to determine the equivalent reactant pressures to which the conditions used there correspond. Afterward, we will carry out more detailed kinetic experiments using a Pt(111) single-crystal surface to directly compare with the other data reported here and to better understand this intermediate pressure kinetic regime.

4. DISCUSSION

Thanks to our operando setup, it has been possible in this work to simultaneously follow the kinetics of the production of the alkane and characterize the evolution of the species present on the surface during the catalytic hydrogenation of ethylene on

dx.doi.org/10.1021/cs300411p | ACS Catal. 2012, 2, 2259−2268

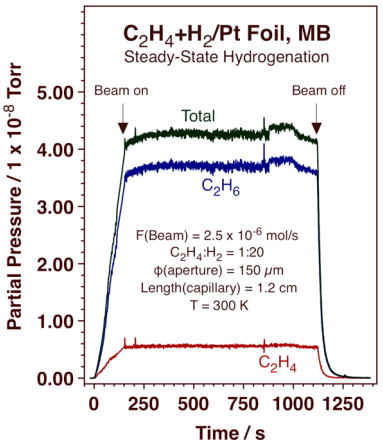

Figure 9. Partial pressures of ethylene and ethane, measured by mass spectrometry, as a function of time for an experiment in which a clean Pt polycrystalline polished disk was exposed to an effusive high-flux collimated beam of a mixture of ethylene and hydrogen. The total flux at the exit of the capillary used to generate the beam was 2.5×10^{-6} mol/s, and the gas composition was a 1:20 H_2/C_2H_4 mixture. About 90% conversion efficiency is observed in this case.

Pt(111) surfaces. Our results corroborate some of the information reported in the past by us and by others. It is well-known that these olefin hydrogenation catalytic processes occur not on the pristine surface of the metal but on a surface covered by carbonaceous deposits. This idea was proposed by Taylor, Thomson, and Webb as early as 1968[16] and demonstrated on Pt(111) by using modern surface-science techniques in 1984.[61] It was inferred then and proven later by in situ IR[49,66,81] and sum-frequency generation (SFG)[47] spectroscopies that, at least with small olefins, the strongly adsorbed carbonaceous layers are based on alkylidyne surface species, ethylidyne ($Pt_3{\equiv}CCH_3$) in the case of ethylene hydrogenation.[46] The formation of ethylidyne on the surface of the Pt(111) surface immediately upon its exposure to the ethylene in the reaction mixture and its persistence throughout the course of the hydrogenation of the olefin were corroborated by the experiments reported here (Figure 4).

It was also shown that the strongly bonded alkylidyne moieties may be hydrogenated under the conditions of the olefin hydrogenation reaction, but at a rate only 1−2 orders of magnitude slower than the turnover frequency of the conversion of gas-phase ethylene to ethane (Figure 5). Evidence for this had been provided in the past by ex situ experiments using a ^{14}C radioisotopic detection technique[63] and also by ex-situ vibrational spectroscopy studies of the removal of the alkylidyne using deuterium labeling.[62,64] It was concluded that these alkylidyne surface species are not direct intermediates in the hydrogenation of olefins but, rather, spectators that play only an indirect role in the reaction by partially passivating the high activity of the clean metal surface and perhaps by intervening in the hydrogen transferring mechanism from the surface to the intermediates in the conversion of the olefins to the alkanes.[3,17,46] Again, those conclusions are borne by the results shown in this report.

In addition to these confirmations of previous reports, a couple of new observations on the behavior of adsorbed alkylidyne layers under hydrogenation catalytic conditions are worth highlighting from our present work. First, it was determined that the frequencies of the vibrational modes associated with the terminal methyl groups and the carbon−carbon bond of those species shift slightly to higher frequencies upon their exposure to atmospheric pressures of hydrogen (Figure 4). This appears to be a general behavior, having been seen here with both normal and perdeutero ethylidyne and also with propylidyne (Table 1). Blue shifts such as these are consistent with a change in the electronic properties of the surface, presumably induced by the reversible coadsorption of atomic hydrogen that occurs in these systems under atmospheric pressures of H_2. It would seem that, under those conditions, the surface becomes more electronegative, leading to stronger C−C and C−H bonds in the terminal methyl moiety of the adsorbed alkylidynes (which acquires slightly more sp^2 character). It is also possible that the bonding of the alkylidynes to the metal surface becomes weaker in the presence of the coadsorbed hydrogen, perhaps facilitating the mobility, or even the temporary partial hydrogenation, of those adsorbates.[46,70] This could explain the viability of the hydrogenation of the π-bonded olefins by the surface, because the motion of the adsorbed alkylidynes may afford the temporary opening of small, naked (H-covered) patches on the metal for such a step.

A second—new and counterintuitive—conclusion from the present work is that the removal of alkylidyne species from the Pt(111) surface is slowed down by increasing coverages of coadsorbed hydrogen. This effect is manifested by the faster alkylidyne removal seen at lower (not higher) hydrogen pressures (Figure 8) and also when the gas-phase hydrogen is mixed with an olefin (as is the case during olefin hydrogenation reactions; Figure 5). Presumably, such crowding of the surface precludes the alkylidyne species from having sufficient space to undergo stepwise hydrogenation and to eventually desorb from the surface. It is known that, under vacuum, ethylidyne can exchange hydrogens for deuteriums at submonoloyer coverages, suggesting that the partial hydrogenation of ethylidyne to ethylidene is feasible on the platinum surface[62,87] and also that the rate of exchange is different if C_2D_4 is used instead of D_2,[87] but it is not clear if those observations can be directly transfer to the atmospheric pressure experiments reported here. In any case, it should be pointed out that this effect is seen only with the adsorbed alkylidyne species; the hydrogenation of the olefins from the gas phase does take place at higher rates with increasing hydrogen pressures.

In terms of the kinetics of olefin conversion on Pt(111), our new data are again fully compatible with previous reports. First, the rate of reaction of ethylene with hydrogen on this catalyst displays approximately zero and first orders with respect to the pressures of the olefin and hydrogen, respectively (Figure 7). Similar kinetic behavior is well-known on supported catalysts[4−6,88] and has also been reported on Pt(111).[61] The most common explanation for this behavior is that the reaction is limited by the dissociative hydrogen adsorption step, which is inhibited by the presence of the alkylidyne layer on the surface. In addition, if deuterium is used instead of normal hydrogen in the reaction mixture, extensive and multiple isotopic scrambling and deuterium incorporation is observed in the products (Figures 2 and 3). This exchange must occur before the formation of the alkane, since such saturated hydrocarbons are quite stable and cannot be activated by the metal under the mild conditions of these hydrogenation reactions. The mechanism for these H-D exchange reactions has been extensively discussed and is believed to involve alkyl surface species.[4,17,22]

dx.doi.org/10.1021/cs300411p | ACS Catal. 2012, 2, 2259−2268

Much surface-science work has been carried out over the years to understand these olefin hydrogenation reactions at a molecular level. That research has led to a fairly complete picture of the reaction mechanism, which involves the indirect participation of alkylidynes or similar strongly adsorbed species. Nevertheless, several aspects of these processes remain unanswered. For one, even though the turnover frequencies reported with practical catalysts are usually quite high, they still correspond to fairly low reaction probabilities. The kinetic rate equations derived under such conditions suggest that these reaction probabilities can be increased by reducing the partial pressure of the olefin, and that idea seems to be borne by the preliminary molecular beam experimental results shown in Figure 9. However, a full characterization of that presumed trend is lacking. Clearly, a change in the behavior of the surface for this type of catalysis needs to occur at intermediate pressures because sustained catalytic olefin hydrogenation is not possible under vacuum conditions.[48] In addition, much remains unexplored about the role of the carbonaceous layers on the kinetics of olefin hydrogenation catalysis. The ability to independently control the nature of the initial alkylidyne surface layer and the reaction mixture, as illustrated here by the use of propylidyne and a $C_2H_4 + H_2$ mixture in Figure 6, offers a new avenue to explore this issue. We are currently following up on these ideas.

Finally, it is important to highlight the power as well as the limitations of operando studies of reaction mechanisms such as those reported here. It was mentioned in the Introduction that the hydrogenation of olefins is believed to involve π-bonded species. However, the detection of such intermediates has been difficult, and a direct correlation of their observation with catalytic activity has not been established.[47] This could be considered a failure, but it needs to be remembered that, in general, reaction intermediates are present in small steady-state concentrations during catalytic conversions and are typically difficult to isolate or detect. Yet, other critical information may be extracted from the in situ characterization of catalytic surfaces relevant to the reaction mechanism and not available by other means. In the case of olefin hydrogenation, much can be learned about the behavior of the carbonaceous deposits present on the surface, the alkylidyne species discussed above, and about their effect on the kinetics of the reaction. A procedure has been outlined here on how the nature of such carbonaceous deposits may be controlled independently from the identity of the reactants to decouple the two effects; this idea will be exploited in the future to correlate the structure of the adsorbates with the hydrogenation activity of the surface. The use of RAIRS is particularly valuable in these operando studies because it is a technique that is relatively easy to implement and that covers a wide range of the vibrational spectra, as needed to obtain unique molecular information.[74]

5. CONCLUSIONS

The catalytic conversion of ethylene with hydrogen on Pt(111) single-crystal surfaces was investigated by simultaneously analyzing the reaction mixture over time with mass spectrometry and following the changes in the surface species using reflection−absorption infrared absorption spectroscopy (RAIRS). Fast conversion of ethylene to ethane and extensive H−D exchange with $C_2H_4 + D_2$ mixtures were seen, with rates and kinetic parameters comparable to those reported in previous publications. The early formation of an almost saturated monolayer of adsorbed alkylidyne and its persistence throughout the catalytic reaction were also confirmed. This alkylidyne layer can be removed from the surface, but at a much slower rate than that of the ethylene-to-ethane conversion. A change in the electronic nature of the platinum surface is nevertheless evident by slight blue shifts in the frequencies of the vibrational modes of the terminal methyl moieties of the alkylidyne when in the presence of an atmosphere containing hydrogen. In addition, increases in hydrogen pressure accelerate the hydrogenation of the ethylene in the gas phase, as expected, but decelerate the removal of the alkylidyne surface species.

The combination of our new mass spectrometry/RAIRS operando capabilities and our separate effusive molecular beam approach to carry out olefin hydrogenation reactions catalytically in a UHV environment offers new opportunities for the further study of these systems to answer some key remaining mechanistic issues. The operando approach will afford the decoupling and independent control of the nature of the alkylidyne layer from the composition of the reaction mixture, whereas the molecular beam setup will permit the exploration of the hydrogenation catalysis in an intermediate pressure regime where high reaction probabilities are expected.

AUTHOR INFORMATION

Corresponding Author

*Email: zaera@ucr.edu.

Present Address

[†]Dartamento de Superficies y Recubrimientos, Instituto de Ciencia de Materiales de Madrid, CSIC, Cantoblanco, 28049 Madrid, Spain.

Notes

The authors declare no competing financial interest.

ACKNOWLEDGMENTS

Funding for this project has been provided by a grant from the U.S. National Science Foundation.

REFERENCES

(1) Davis, S. M.; Zaera, F.; Somorjai, G. A. *J. Catal.* **1982**, *77*, 439.
(2) Somorjai, G. A. *CATTECH* **1999**, *3*, 84.
(3) Ma, Z.; Zaera, F. *Surf. Sci. Rep.* **2006**, *61*, 229.
(4) Bond, G. C. *Metal-Catalysed Reactions of Hydrocarbons*; Springer: New York, 2005.
(5) Horiuti, J.; Miyahara, K. *Hydrogenation of Ethylene on Metallic Catalysts; NSRDS-NBC No. 13*; National Bureau of Standards: Washington, DC, 1968.
(6) Schlatter, J. C.; Boudart, M. *J. Catal.* **1972**, *24*, 482.
(7) Twigg, G. H. *Discuss. Faraday Soc.* **1950**, *8*, 152.
(8) Taylor, T. I. Hydrogen Isotopes in the Study of Hydrogenation and Exchange. In *Catalysis*; Emmett, P. H., Ed.; Reinhold: New York, 1957; Vol. 5, pp 257−403.
(9) Tétényi, P.; Guczi, L.; Sárkány, A. *Acta Chim. Acad. Sci. Hung.* **1978**, *97*, 221.
(10) Polanyi, M.; Horiuti, J. *Trans. Faraday Soc.* **1934**, *30*, 1164.
(11) Zaera, F. *Top. Catal.* **2005**, *34*, 129.
(12) Morales, R.; Zaera, F. *J. Phys. Chem. B* **2006**, *110*, 9650.
(13) Taylor, G. F.; Thomson, S. J.; Webb, G. *J. Catal.* **1968**, *12*, 191.
(14) Sheppard, N. *Annu. Rev. Phys. Chem.* **1988**, *39*, 589.
(15) Wang, P.-K.; Slichter, C. P.; Sinfelt, J. H. *J. Phys. Chem.* **1985**, *89*, 3606.
(16) Thomson, S. J.; Webb, G. *J. Chem. Soc., Chem. Commun.* **1976**, 526.
(17) Zaera, F. *Catal. Lett.* **2003**, *91*, 1.

(18) Somorjai, G. A. *Chemistry in Two Dimensions: Surfaces*; Cornell University Press: Ithaca, 1981.
(19) Albert, M. R.; Yates, J. T., Jr. *The Surface Scientist's Guide to Organometallic Chemistry*; American Chemical Society: Washington, DC, 1987.
(20) Zaera, F. *Prog. Surf. Sci.* **2001**, *69*, 1.
(21) Salmerón, M.; Somorjai, G. A. *J. Phys. Chem.* **1982**, *86*, 341.
(22) Zaera, F. *J. Phys. Chem.* **1990**, *94*, 5090.
(23) Kesmodel, L. L.; Dubois, L. H.; Somorjai, G. A. *Chem. Phys. Lett.* **1978**, *56*, 267.
(24) Skinner, P.; Howard, M. W.; Oxton, I. A.; Kettle, S. F. A.; Powell, D. B.; Sheppard, N. *J. Chem. Soc., Faraday Trans. II* **1981**, *77*, 1203.
(25) Koestner, R. J.; Frost, J. C.; Stair, P. C.; Van Hove, M. A.; Somorjai, G. A. *Surf. Sci.* **1982**, *116*, 85.
(26) Creighton, J. R.; White, J. M. *Surf. Sci.* **1983**, *129*, 327.
(27) Zhou, X. L.; Liu, Z. M.; White, J. M. *Chem. Phys. Lett.* **1992**, *195*, 618.
(28) Zaera, F.; Bernstein, N. *J. Am. Chem. Soc.* **1994**, *116*, 4881.
(29) Janssens, T. V. W.; Zaera, F. *Surf. Sci.* **1995**, *344*, 77.
(30) Cremer, P.; Stanners, C.; Niemantsverdriet, J. W.; Shen, Y. R.; Somorjai, G. *Surf. Sci.* **1995**, *328*, 111.
(31) Janssens, T. V. W.; Zaera, F. *J. Phys. Chem.* **1996**, *100*, 14118.
(32) Brown, W. A.; Kose, R.; King, D. A. *Surf. Sci.* **1999**, *440*, 271.
(33) Deng, R.; Herceg, E.; Trenary, M. *Surf. Sci.* **2004**, *560*, L195.
(34) Andersin, J.; Lopez, N.; Honkala, K. *J. Phys. Chem. C* **2009**, *113*, 8278.
(35) Zhao, Z.-J.; Moskaleva, L. V.; Aleksandrov, H. A.; Basaran, D.; Rösch, N. *J. Phys. Chem. C* **2010**, *114*, 12190.
(36) Li, M.; Guo, W.; Jiang, R.; Zhao, L.; Lu, X.; Zhu, H.; Fu, D.; Shan, H. *J. Phys. Chem. C* **2010**, *114*, 8440.
(37) Aleksandrov, H. A.; Moskaleva, L. V.; Zhao, Z.-J.; Basaran, D.; Chen, Z.-X.; Mei, D.; Rösch, N. *J. Catal.* **2012**, *285*, 187.
(38) Zaera, F.; Janssens, T. V. W.; Öfner, H. *Surf. Sci.* **1996**, *368*, 371.
(39) Zaera, F.; French, C. R. *J. Am. Chem. Soc.* **1999**, *121*, 2236.
(40) Pallassana, V.; Neurock, M.; Lusvardi, V. S.; Lerou, J. J.; Kragten, D. D.; van Santen, R. A. *J. Phys. Chem. B* **2002**, *106*, 1656.
(41) Stacchiola, D.; Tysoe, W. T. *J. Phys. Chem. C* **2009**, *113*, 8000.
(42) Lykhach, Y.; Staudt, T.; Tsud, N.; Skala, T.; Prince, K. C.; Matolin, V.; Libuda, J. *Phys. Chem. Chem. Phys.* **2011**, *13*, 253.
(43) Demuth, J. E. *Surf. Sci.* **1979**, *84*, 315.
(44) Stuve, E. M.; Madix, R. J. *J. Phys. Chem.* **1985**, *89*, 3183.
(45) Zaera, F. *Chem. Rev.* **1995**, *95*, 2651.
(46) Zaera, F. *Langmuir* **1996**, *12*, 88.
(47) Cremer, P. S.; Su, X.; Shen, Y. R.; Somorjai, G. A. *J. Am. Chem. Soc.* **1996**, *118*, 2942.
(48) Öfner, H.; Zaera, F. *J. Phys. Chem. B* **1997**, *101*, 396.
(49) Ohtani, T.; Kubota, J.; Kondo, J. N.; Hirose, C.; Domen, K. *J. Phys. Chem. B* **1999**, *103*, 4562.
(50) Neurock, M.; Pallassana, V.; van Santen, R. A. *J. Am. Chem. Soc.* **2000**, *122*, 1150.
(51) Hugenschmidt, M. B.; Dolle, P.; Jupille, J.; Cassuto, A. *J. Vac. Sci. Technol. A* **1989**, *7*, 3312.
(52) Neurock, M.; van Santen, R. A. *J. Phys. Chem. B* **2000**, *104*, 11127.
(53) Zaera, F.; Chrysostomou, D. *Surf. Sci.* **2000**, *457*, 71.
(54) Lee, I.; Zaera, F. *J. Phys. Chem. C* **2007**, *111*, 10062.
(55) Öfner, H.; Zaera, F. *J. Am. Chem. Soc.* **2002**, *124*, 10982.
(56) Blakely, D. W.; Kozak, E. I.; Sexton, B. A.; Somorjai, G. A. *J. Vac. Sci. Technol.* **1976**, *13*, 1091.
(57) Rodriguez, J. A.; Goodman, D. W. *Surf. Sci. Rep.* **1991**, *14*, 1.
(58) Wilson, J.; Guo, H.; Morales, R.; Podgornov, E.; Lee, I.; Zaera, F. *Phys. Chem. Chem. Phys.* **2007**, *9*, 3830.
(59) Kahn, D. R.; Petersen, E. E.; Somorjai, G. A. *J. Catal.* **1974**, *34*, 294.
(60) Davis, S. M.; Somorjai, G. A. *J. Catal.* **1980**, *65*, 78.
(61) Zaera, F.; Somorjai, G. A. *J. Am. Chem. Soc.* **1984**, *106*, 2288.
(62) Koel, B. E.; Bent, B. E.; Somorjai, G. A. *Surf. Sci.* **1984**, *146*, 211.
(63) Davis, S. M.; Zaera, F.; Gordon, B.; Somorjai, G. A. *J. Catal.* **1985**, *92*, 240.
(64) Wieckowski, A.; Rosasco, S. D.; Salaita, G. N.; Hubbard, A.; Bent, B. E.; Zaera, F.; Godbey, D.; Somorjai, G. A. *J. Am. Chem. Soc.* **1985**, *107*, 5910.
(65) Cremer, P. S.; Su, X.; Somorjai, G. A.; Shen, Y. R. *J. Mol. Catal. A: Chem.* **1998**, *131*, 225.
(66) Beebe, T. P., Jr.; Yates, J. T., Jr. *J. Am. Chem. Soc.* **1986**, *108*, 663.
(67) Ko, M. K.; Frei, H. *J. Phys. Chem. B* **2004**, *108*, 1805.
(68) Zaera, F. *J. Phys. Chem. B* **2002**, *106*, 4043.
(69) Zaera, F. *Appl. Catal., A* **2002**, *229*, 75.
(70) Marsh, A. L.; Somorjai, G. A. *Top. Catal.* **2005**, *34*, 121.
(71) Hoffmann, H.; Griffiths, P. R.; Zaera, F. *Surf. Sci.* **1992**, *262*, 141.
(72) Lee, I.; Nguyen, M. K.; Morton, T. H.; Zaera, F. *J. Phys. Chem. C* **2008**, *112*, 14117.
(73) Hoffmann, F. M. *Surf. Sci. Rep.* **1983**, *3*, 107.
(74) Zaera, F. *Int. Rev. Phys. Chem.* **2002**, *21*, 433.
(75) Loaiza, A.; Zaera, F. *J. Am. Soc. Mass Spectrom.* **2004**, *15*, 1366.
(76) Amenomiya, Y.; Pottie, R. F. *Can. J. Chem.* **1968**, *46*, 1741.
(77) Stenhagen, E.; Abrahamson, S.; McLafferty, F. *Registry of Mass Spectral Data*; Wiley-Interscience: New York, 1974.
(78) Loaiza, A.; Xu, M.; Zaera, F. *J. Catal.* **1996**, *159*, 127.
(79) Malik, I. J.; Brubaker, M. E.; Trenary, M. *J. Electron Spectrosc. Relat. Phenom.* **1987**, *45*, 57.
(80) Chesters, M. A.; De La Cruz, C.; Gardner, P.; McCash, E. M.; Pudney, P.; Shahid, G.; Sheppard, N. *J. Chem. Soc., Faraday Trans.* **1990**, *86*, 2757.
(81) Mims, C. A.; Weisel, M. D.; Hoffmann, F. M.; Sinfelt, J. H.; White, J. M. *J. Phys. Chem.* **1993**, *97*, 12656.
(82) Chrysostomou, D.; French, C.; Zaera, F. *Catal. Lett.* **2000**, *69*, 117.
(83) Lee, I.; Albiter, M. A.; Zhang, Q.; Ge, J.; Yin, Y.; Zaera, F. *Phys. Chem. Chem. Phys.* **2011**, *13*, 2449.
(84) Brandt, B.; Fischer, J.-H.; Ludwig, W.; Schauermann, S.; Libuda, J.; Zaera, F.; Freund, H.-J. *J. Phys. Chem. C* **2008**, *112*, 11408.
(85) Brandt, B.; Ludwig, W.; Fischer, J. H.; Libuda, J.; Zaera, F.; Schauermann, S. *J. Catal.* **2009**, *265*, 191.
(86) Guevremont, J. M.; Sheldon, S.; Zaera, F. *Rev. Sci. Instrum.* **2000**, *71*, 3869.
(87) Janssens, T. V. W.; Stone, D.; Hemminger, J. C.; Zaera, F. *J. Catal.* **1998**, *177*, 284.
(88) Farkas, A.; Farkas, L. *J. Am. Chem. Soc.* **1938**, *60*, 22.